PCP
PLANT & CELL PHYSIOLOGY

Regular Paper

Thermomorphogenesis of the *Arabidopsis thaliana* Root: Flexible Cell Division, Constrained Elongation and the Role of Cryptochrome

Maura J. Zimmermann[1,2,3], Vikram D. Jathar[2] and Tobias I. Baskin[2,*]

[1]Plant Biology Program, University of Massachusetts, Amherst, MA 01003, USA
[2]Department of Biology, University of Massachusetts, Amherst, MA 01003, USA
[3]Present address: School of Integrative Plant Sciences, Cornell University, Ithaca, NY 14853, USA.
*Corresponding author: E-mail, baskin@umass.edu
(Received 21 March 2024; Accepted 19 July 2024)

Understanding how plants respond to temperature is relevant for agriculture in a warming world. Responses to temperature in the shoot have been characterized more fully than those in the root. Previous work on thermomorphogenesis in roots established that for *Arabidopsis thaliana* (Columbia) seedlings grown continuously at a given temperature, the root meristem produces cells at the same rate at 15°C as at 25°C and the root's growth zone is the same length. To uncover the pathway(s) underlying this constancy, we screened 34 *A. thaliana* genotypes for parameters related to growth and division. No line failed to respond to temperature. Behavior was little affected by mutations in phytochrome or other genes that underly thermomorphogenesis in shoots. However, a mutant in cryptochrome 2 was disrupted substantially in both cell division and elongation, specifically at 15°C. Among the 34 lines, cell production rate varied extensively and was associated only weakly with root growth rate; in contrast, parameters relating to elongation were stable. Our data are consistent with models of root growth that invoke cell non-autonomous regulation for establishing boundaries between meristem, elongation zone and mature zone.

Keywords: *Arabidopsis thaliana* ● Cell production rate ● Cryptochrome 2 ● Growth-zone length ● Kinematic analysis ● Meristem length ● Relative elongation

Editor-in-Chief's Choice

Introduction

How does temperature affect a plant root? We ask this question in part because of the peril of climate change. But we ask also because temperature, imbuing air and water with energy, sets the tempo of chemical reactions; hence, metabolic networks no less than ecosystems are vulnerable to temperature change. Among endotherms, the metabolic clockwork is protected by confining cells to a narrow temperature range; cells of an endotherm exceeding the range by even a few degrees are damaged or killed. By contrast, plants allow their cells to change temperatures by tens of degrees, even within an hour; the cells may suffer little if any damage. In plants, metabolism is engineered to accommodate rapidly changing reaction rates. Studying how plants respond to temperature, while necessary for sustaining agricultural productivity, is also fascinating.

Collectively, physiological and developmental responses to temperature are called thermomorphogenesis (Stoller and Woolley 1983, Casal and Balasubramanian 2019). The word was coined by analogy to the popular term, photomorphogenesis, which describes responses to light. Just as photomorphogenesis includes responses to dim and bright light, so too thermomorphogenesis includes responses to low and high temperatures. Recently, some authors have redefined thermomorphogenesis to mean responses to warm or hot temperatures only (e.g. Hayes et al. 2021). Indeed, in the face of climate change, responses to higher-than-usual temperatures are salient, and high temperatures induce a suite of specific responses (Hatfield and Prueger 2015, Gray and Brady 2016). Nevertheless, developmental responses to cool temperatures also occur. We will use thermomorphogenesis in its original sense to mean responses induced by temperature, whether warm or cool.

Specifically, our work concerns how the root, in response to changing temperature, acclimates cell division and expansion. These processes are fundamental for morphogenesis as well as for physiological responses to the environment. Under temperature extremes, growth stops while the plant strives to curtail the damage and survive. Without growth, there is little morphogenesis. Therefore, we study temperatures that are moderate. Defining 'moderate' explicitly is difficult; however, conceptually we may follow Aristotle's definition of virtue as being intermediate between extremes (e.g. cowardice < bravery > rashness). Temperature extremes are stresses and they decrease fitness

Plant Cell Physiol. 65(9): 1434–1449 (2024) doi:https://doi.org/10.1093/pcp/pcae082, Advance Access publication on 20 July 2024, available online at https://academic.oup.com/pcp

(Zhang et al. 2021). By contrast, plants can acclimate to intermediate temperatures, maintaining fitness. Indeed, a temperature range over which fitness stays constant is a workable definition of 'moderate'. For *Arabidopsis thaliana*, this range has been shown to be approximately from 15°C to 25°C (Ibañez et al. 2017).

In response to changing temperature, cell division and elongation in the root acclimate in possibly counterintuitive ways. Comparing plants (Columbia background) germinated and grown continuously at the tested temperature, the root meristem is longer but less active at 15°C compared to 25°C (Yang et al. 2017). These trends balance so that the total rate at which cortical cells are produced by the root meristem at 15°C and 25°C is indistinguishable. Furthermore, at these temperatures, the length of the root's growth zone (i.e. meristem plus elongation zone) is also essentially the same. By contrast, developmental processes in both roots and shoots typically speed up or slow down with temperature (Parent and Tardieu 2012). The approximate constancy of cell production rate and growth-zone length across the moderate temperature range implies specific acclimation.

Concerning this acclimation, what are the responsible pathway(s)? For shoots, starring in thermomorphogenesis are phytochrome and its associated transcription factor, phytochrome-interacting factor 4 (PIF4; Casal and Balasubramanian 2019, Noguchi and Kodama 2022, Samtani et al. 2022). Playing supporting roles are components of the circadian clock, such as early flowering 3 (ELF3; Thines et al. 2010). By contrast, in roots, pathways based on phytochrome and circadian clock components are apparently inactive (Martins et al. 2017, Bellstaedt et al. 2019, Gaillochet et al. 2020, Lee et al. 2021, Borniego et al. 2022, Ai et al. 2023). Conceivably, signaling from phytochrome is dampened in the shallow root system of *A. thaliana* to avoid significant plastid greening, although the roots do synthesize measurable, albeit tiny, quantities of chlorophyll in the light (Usami et al. 2004). Instead, root thermomorphogenesis appears to depend partly on auxin and brassinosteroids; but, specific pathways remain to be delineated (Martins et al. 2017, Bellstaedt et al. 2019, Ai et al. 2023).

To find active participants in root thermomorphogenesis, we screened 34 genotypes, including several accessions and mutants in plausibly relevant genes. To characterize morphogenesis, we assayed cell division and elongation by means of kinematics (Silk 1984, Baskin 2013). We report here that cell division is flexible: only a few lines retain the temperature-invariant cell production rate typifying Columbia. By contrast, elongation parameters are steadfast, with all lines but one having meristem length, growth-zone length and relative elongation rate behaving similarly to those of Columbia. The exception is a mutant in cryptochrome 2 that is specifically and strongly defective at 15°C. These results identify this blue-light photoreceptor as a player in root thermomorphogenesis and, in general, highlight the significance of elongation processes in governing the responsiveness of roots to their environment.

Results

Overview

To elucidate the pathway(s) used by the root to respond to moderate temperatures, we compare plants grown at 15°C versus 25°C; these temperatures have been shown to have little effect on *A. thaliana* fitness (Ibañez et al. 2017). To avoid time-dependent changes in growth rate and superimposing changes due to temperature with those due to circadian rhythms, we grow plants under continuous light (as did Yang et al. 2017). Finally, to avoid responses induced by changing conditions abruptly, we compare plants grown from germination onward continuously at each temperature.

We assayed plants grown at 25°C on day 7 and at 15°C on day 14, when the root growth rate had reached a roughly steady state (Yang et al. 2017). At 15°C, roots of some genotypes did not reach a steady state by day 14; nevertheless, that day was used for the 15°C treatment because it represents the equivalent thermal time as day 7 at 25°C. Steady-state growth simplifies kinematic calculations and minimizes the interference from variations in the time of germination.

We screened 34 genotypes, which we have divided into three classes. First are 'accessions', some common and others reported to respond to temperature unusually. Included in the accessions group for the sake of ready comparison is *er-105*, a Columbia line that like Ler has a knocked-out erecta kinase (Torii et al. 1996). Second are 'photobiology' related, which includes mutants in phytochrome and other photoreceptors; and third are 'developmental', which includes mainly mutants in genes involved in hormonal responses. Members of the latter two classes are all in the Columbia background, except for *spy-8* and a phytochrome quintuple mutant (*phyQ*), which are in Ler. Brief descriptions of each line and a reference are given in **Supplementary Table S1**.

Our screen is divided into two parts, corresponding to the two temperature-invariant processes reported previously, namely, cell production rate and growth-zone length (Yang et al. 2017). We present results of the first part in three sections ('root growth rate', 'mature cortical cell length' and 'cell production rate') followed by results for the second part in a single section ('elongation parameters'; so called because, in addition to growth-zone length, we measured the length of the meristem and the rate of relative elongation within the elongation zone).

Root growth rate

For part one, we measured root growth rate and mature cortical cell length and then calculated cell production rate based on the kinematic relationship illustrated in **Fig. 1**. Briefly, at steady state, the time to deposit a mature cell into the elongation zone equals the length of that cell divided by the velocity of the root tip (i.e. root growth rate); that time is the same as needed by the meristem to deposit a cell into the elongation zone. The reciprocal of this time gives the rate at which the meristem produces cells (Silk et al. 1989).

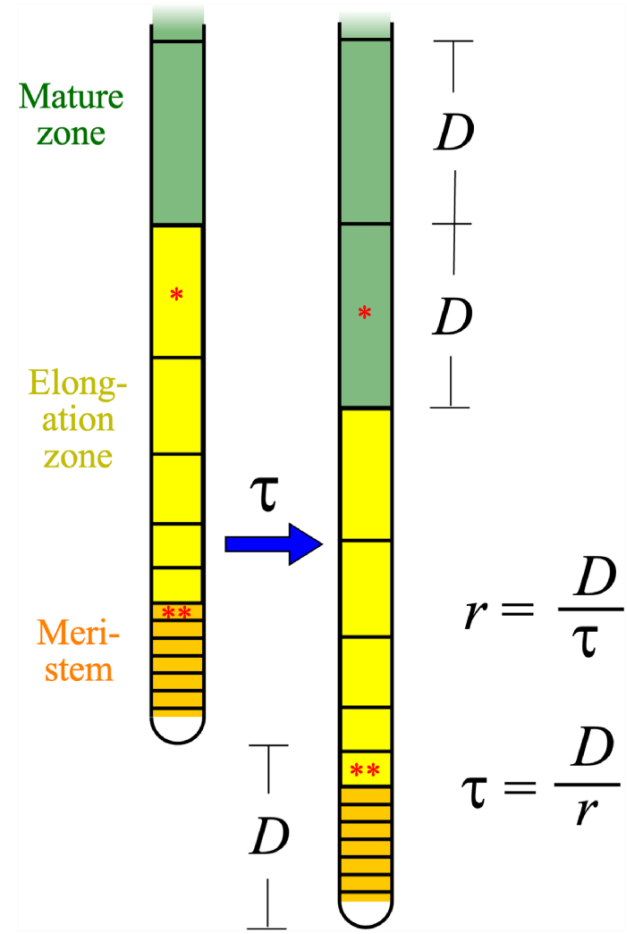

Fig. 1 Diagram illustrating the screen for cell production rate. The root is schematized as a single cell file, with the indicated zones. At steady state, in time τ, the root grows a distance, D, that is equal to the length of a mature cell. During that time, the last cell of the elongation zone (*) attains its mature length ($=D$) and exits from the elongation zone; concomitantly, the last cell of the meristem (**) enters the elongation zone. Thus, this meristem is producing 1 cell per τ time units. To find time τ, we divide the average length of a root's mature cortex cells, D, by that root's growth rate, r. We call the reciprocal of this time ($1/\tau$) cell production rate: this value represents how fast cells are produced by a file of cortex cells (Silk et al. 1989).

Under our conditions, Columbia roots grew about twice as fast at 25°C than at 15°C (**Fig. 2**). For ease of comparison, the Columbia rate and standard deviation are represented by a long vertical band centered on the mean for each temperature. Roots of all of the genotypes responded to temperature, clearly growing faster at 25°C than at 15°C. Many lines resembled Columbia at each temperature including *pif4*, *elf3* and *phyQ*. Notably for these lines, the corresponding genes underlie thermomorphogenesis in shoots (Casal and Balasubramanian 2019). Consistently, PIF4, ELF3 and phytochrome have been previously reported to play little, if any, role in the root's growth response to temperature (Martins et al. 2017, Bellstaedt et al. 2019, Gaillochet et al. 2020, Lee et al. 2021, Borniego et al. 2022, Ai et al. 2023). However, the previous work considered elevated temperature; our work extends the temperature range to 15°C where root thermomorphogenesis is apparently oblivious to PIF4 and related pathway components.

Many of the lines grew somewhat faster or slower than Columbia at one or both temperatures. Although some of these differences were significant statistically, their biological significance is uncertain. The data in **Fig. 2** were obtained over several years and despite apparently constant conditions, even Columbia on some days grew a little faster or slower. However, several lines deviated substantially from Columbia. At both temperatures, Cvi, *shy2* and *bes1-D* grew more slowly than Columbia, suggesting that these lines differ generally in their growth capacities. A group of lines grew particularly slowly at 15°C (*pif5*, *spy* and *cry2*). In this regard, *cry2* stood out, having the slowest growth of any line at 15°C and yet growing at the same rate as Columbia at 25°C. To our knowledge, this is the first report suggesting cryptochrome 2 is involved in thermomorphogenesis in roots.

To represent overall temperature responsiveness, we calculated the ratio of growth rate at 25°C to 15°C. Because the temperature interval is 10°, we call this ratio a Q_{10} value, although in the physiological literature, Q_{10} values are typically attached to short-term effects, obtained by transferring material between temperatures (Larigauderie and Körner 1995, Zimmermann et al. 2022). The Q_{10} values for root growth rate highlight lines with unusual overall temperature sensitivity (**Fig. 3**). Most lines had a value around 2, typical of biological responses. In contrast, three lines (*pif5*, *spy-3* and *spy-8*) clustered around a Q_{10} value of 4 and *cry2* had a value near 7. These results identify contributions to root thermomorphogenesis from PIF5, SPY and CRY2, based mainly on slower-than-expected growth at 15°C.

Mature cortical cell length

In the same trials used to measure root growth rate, we measured the length of mature cortical cells (**Fig. 4**). As expected for Columbia from previous work (Yang et al. 2017, Zimmermann et al. 2022), mature cortical cells at 25°C were about twice as long as those at 15°C (210 versus 110 μm). A rough doubling also occurred in four of the accessions, six of the photobiology mutants and four of the developmental mutants (**Fig. 4**).

However, for around half of the genotypes, mature cortical cell length did not resemble that of Columbia. Cell lengths for one group of lines were similar at both temperatures, resembling that of Columbia at 25°C; this group includes two accessions (Mt and Cvi) and four photobiology mutants (*phot1*, *phot1/phot2*, *cry2* and *PIF4-OE*). Conversely, cell lengths for another group of lines were more or less the same at both temperatures but similar to Columbia at 15°C; this group includes the Ler accession and *er-105*, four photobiology mutants (*pif1*, *pif5*, *pif4/5* and *phyQ*) and four of the developmental mutants (*shy2*, *bzr1-1D*, *ahk3* and *arr1/arr12*). For convenience, we will refer to the former as the 'long-cell' phenotype and to the latter as the 'short-cell' phenotype.

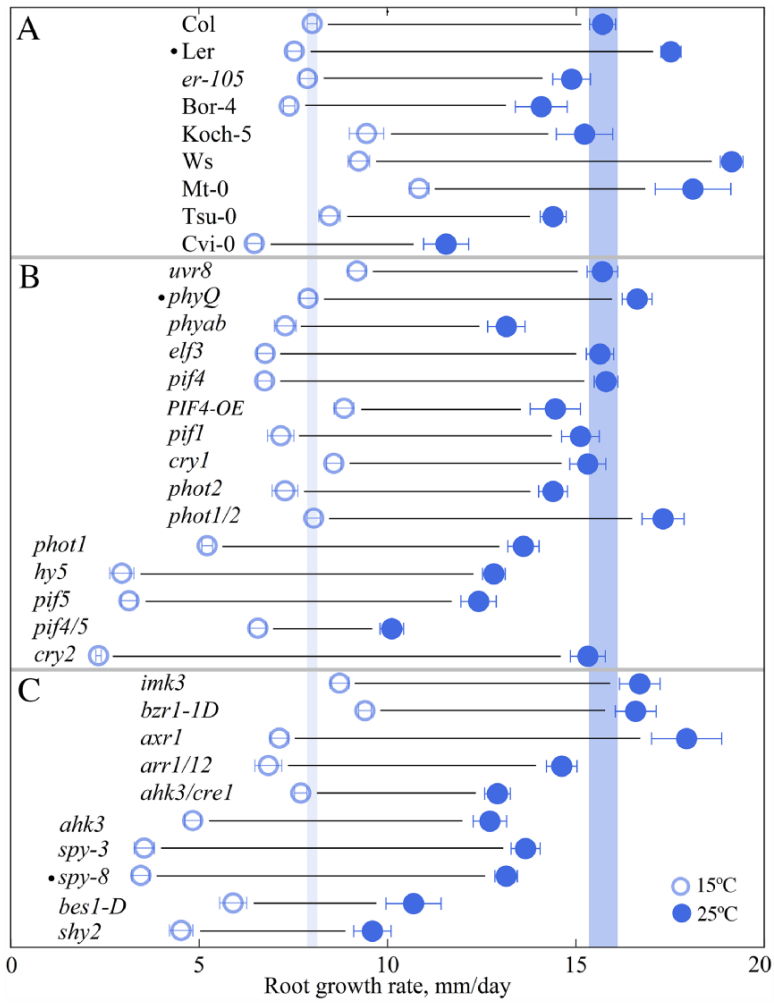

Fig. 2 Root growth rate at 15°C and 25°C for the indicated genotypes. (A) Accessions. Included in this group is *er-105* for comparison to Ler (*er-105* is in the Columbia background but like Ler is null for erecta). (B) Photobiology related lines. (C) Developmental lines. In B and C, all lines are in Columbia except *phy*Q and *spy-8*, which are in Ler (indicated by the filled circle). Symbols show mean ± SD. Vertical bands are centered at the mean for Columbia and are as wide as the SD. Sample sizes and brief descriptions of the lines are given in **Supplementary Table S1**.

Two other patterns occurred. In *ahk3*/*cre1*, mature cortical cells were nearly the same length at both temperatures, but this length was in between that of Columbia at 15°C and 25°C. In two lines (*bes1-D* and *cry1*), mature cell length at 15°C was notably longer than it was at 25°C, inverting the usual relationship. Mature cells of *cry1* at 15°C were about 2.5 times longer than those of Columbia, offering further support for an involvement of cryptochrome in thermomorphogenesis in roots. Overall, the length of mature cells appears to be determined with considerable flexibility.

The temperature sensitivity of mature cortical cell length is illustrated by the range of Q_{10} values (**Fig. 3**). Only the Bor accession matched exactly the near doubling seen in Columbia (i.e. Q_{10} near 2). No line had a Q_{10} value greater than 2. In two lines, mature cells actually shortened (*cry1* and *bes1-D*) (i.e. Q_{10} less than 1). Consistent with either a short-cell or long-cell phenotype, many lines had Q_{10} values close to 1, meaning that mature cell length was essentially insensitive to temperature. The similarity at both temperatures among so many genotypes suggests that mature cell length is regulated specifically. As for root thermomorphogenesis pathways, the cell length results implicate various proteins (erecta, spindly, phototropin and crypotochrome), but their roles might be indirect.

Cortical cell production rate

Having measured both root growth rate and mature cell length, we calculated cell production rate (**Fig. 1**). This rate is the ratio of root growth rate to mature cell length and represents the cumulative output of cells, per file, rather than a rate of cell division (Green 1976, Silk et al. 1989, Baskin 2013). In the trials shown in Figs. 2 and 4, root growth rate and mature cortical cell length were measured on the same roots, thereby enabling cell production rate to be obtained on an individual root basis. With temperature increasing both root growth rate and mature cell length to about the same extent, cell production rate in

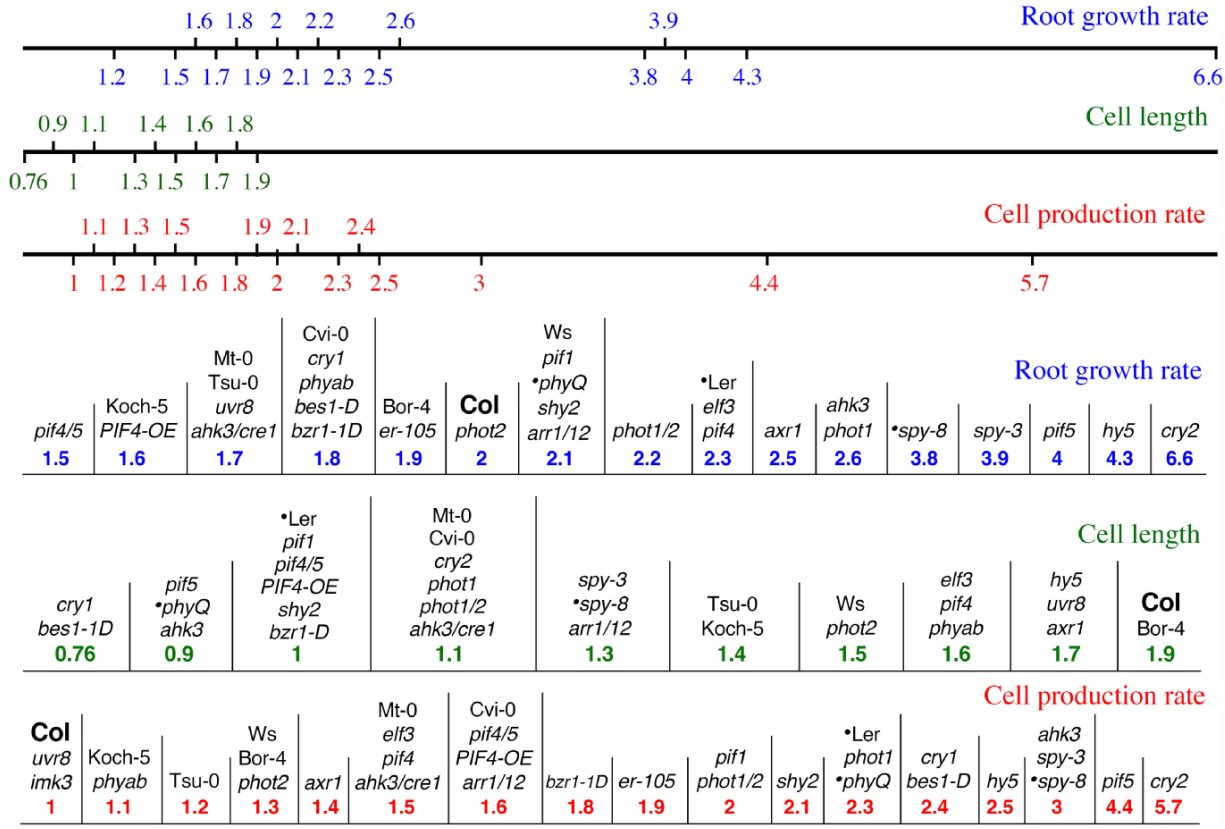

Fig. 3 Steady state Q_{10} values. Values on the number lines (top) and table of genotypes (below) are the ratio of the given parameter at 25°C divided by its value at 15°C. Values used are the means from **Figs. 2**, **4**, **5**. Number lines (top) are all drawn to the same scale. Values for Columbia (Col) are shown in black; genotypes in the Ler background are preceded by a filled circle.

Columbia roots was indistinguishable at both temperatures (**Fig. 5**), as reported previously (Yang et al. 2017, Zimmermann et al. 2022).

Among the genotypes screened, only three (*uvr8*, *phyab* and *imk3*) had cell production rates as tightly matched at the two temperatures as had Columbia. Eight lines produced cells at 25°C notably faster than did Columbia but with little or modest effect at 15°C (*Ler*, *er-105*, *pif1*, *phyQ*, *arr1/arr12*, *bzr1-1D* and *ahk3*). A larger group of lines produced cells at 15°C more slowly than did Columbia and with little or modest effect at 25°C. Again, *cry2* stood out among the lines as having the slowest rate of cell production at 15°C. The accession Cvi produced cells more slowly than did Columbia at both temperatures; results, along with its slow root growth rate at both temperatures, imply a basis in development rather than in temperature response.

In general, cell production rate varied extensively with temperature (**Fig. 5**). Decreased cell production rate specifically at 15°C was sometimes but not invariably associated with the long-cell phenotype. Likewise, in some cases, the stepped-up rate at 25°C was accompanied by the short cell phenotype, but not always. The lability of cell production rate as a function of temperature is apparent from the Q_{10} values, which were spread out between 1 to 2.5 (**Fig. 3**). Certain lines had notably higher values, with *cry2* reaching 5.7. Based on the strength of the response, it is reasonable to conclude that how rapidly cells divide in the root meristem in response to temperature is influenced by AHK3, SPY, PIF5, CRY2 and erecta, but as with cell length, this influence might be indirect.

Elongation parameters

For the second part of our screen, we assayed elongation parameters: namely, relative elongation rate (of the elongation zone), meristem length and growth-zone length. We were unable to screen all 34 genotypes because the assay for elongation parameters is time-consuming. We obtained these elongation parameters from the spatial profile of velocity. The velocity profile captures underlying elongation because velocity (i.e. movement) is caused by growth (Silk 1984, Baskin and Zelinsky 2019).

In general, the velocity profile for a root is roughly sigmoidal, with two regions of gradual change surrounding a region of steep change (**Fig. 6**). As described in the Materials and Methods, we fitted a modified sigmoid function to the velocity profile for each root. This function was chosen because it parameterizes the center points of the two transitions as well as the slope of the steep region. We define the distance from the quiescent center to the first transition point as 'meristem length'; in fact, that length includes a transitional region in which cells no longer divide (Yang et al. 2017). We define the

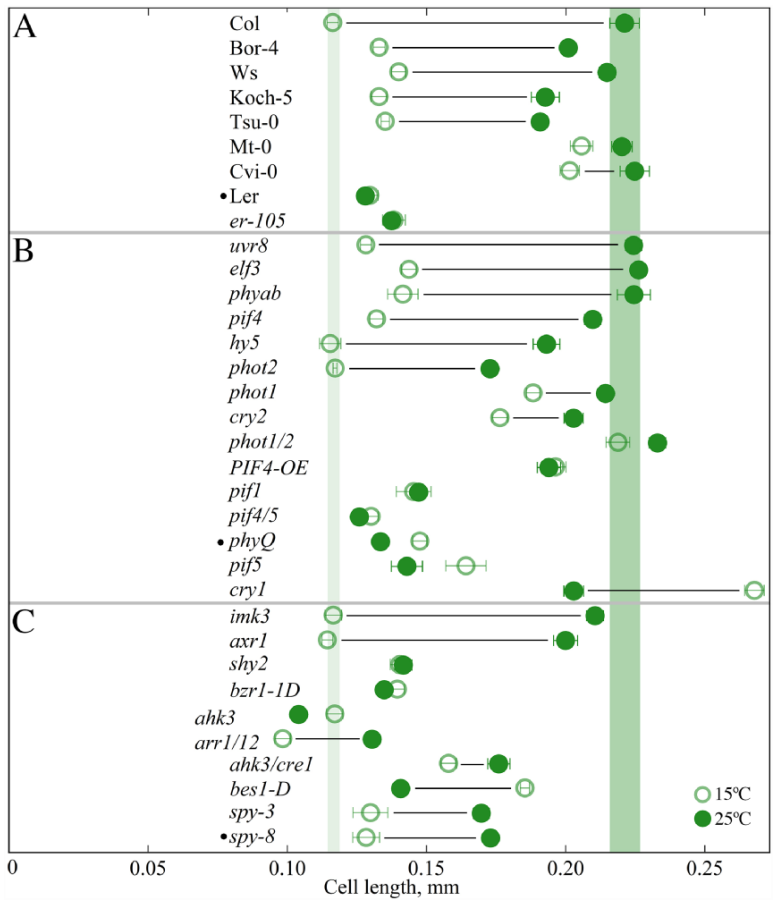

Fig. 4 Mature cortical cell length for the indicated genotypes. (A) Accessions. (B) Photobiology related lines. (C) Developmental lines. Symbols show mean ± SD. Vertical bands are centered at the mean for Columbia and are as wide as the SD. Line names preceded by a filled circle are in the Ler background.

distance from the quiescent center to the second transition point as 'growth-zone length'; this length spans both the meristem and elongation zone. Finally, we define the slope of the steep, nearly linear portion of the sigmoid as 'relative elongation rate'. This parameter is sometimes called 'cell elongation rate'; however, the elongation process is subcellular (Green 1976, Silk 1984, Baskin 2013). By whatever name, the parameter quantifies the process of elongation.

In Columbia as reported previously (Yang et al. 2017), relative elongation rate at 25°C was about 1.75 times greater than that at 15°C (**Fig. 7**). In all lines, relative elongation rate behaved similarly. Note that even for *cry2* at 15°C, where root growth rate decreased by about 80%, relative elongation rate decreased by only about 20%. Evidently, in these diverse genotypes, the elongation machinery (e.g. cell wall deposition and loosening) responds to temperature via pathways that are essentially independent of the tested genes.

We also measured meristem length (+transition zone). In Columbia, the meristem was about 30% longer at the cooler temperature than at the warmer (**Fig. 8**), similar to previous reports (Martins et al. 2017, Yang et al. 2017, Borniego et al. 2022). A lengthened meristem at 15°C is surprising because at each temperature cells are produced at the same rate. A similarly enlarged meristem at 15°C characterized nearly all of the lines. In *shy2*, the difference was smaller than the others, and in *phot1/2*, the difference was larger (**Fig. 8**). In general, a shorter meristem at the warmer temperature appears to be a robust response. However, the exception was *cry2*, whose meristem at 15°C actually trended shorter than at 25°C.

Finally, we measured the length of the growth zone (i.e. the distance from the quiescent center to where growth ceased). In Columbia, the length was similar at both temperatures, although slightly longer at the cooler temperature (**Fig. 9**). In nearly all lines, the growth zone had essentially the same length at both temperatures. Again, the exception was *cry2*, where the growth zone was strikingly short specifically at 15°C. Taken together, elongation parameters in thermomorphogenesis appear stable; and cryptochrome 2 appears to play an important role in promoting elongation at 15°C.

Mechanistically, the magnitude of root growth rate depends on both relative elongation rate and growth-zone length. To compare the contribution of each, we plotted root growth rate versus growth-zone length and versus relative elongation rate (**Fig. 10**). For the example genotype shown (*pif5* at 25°C),

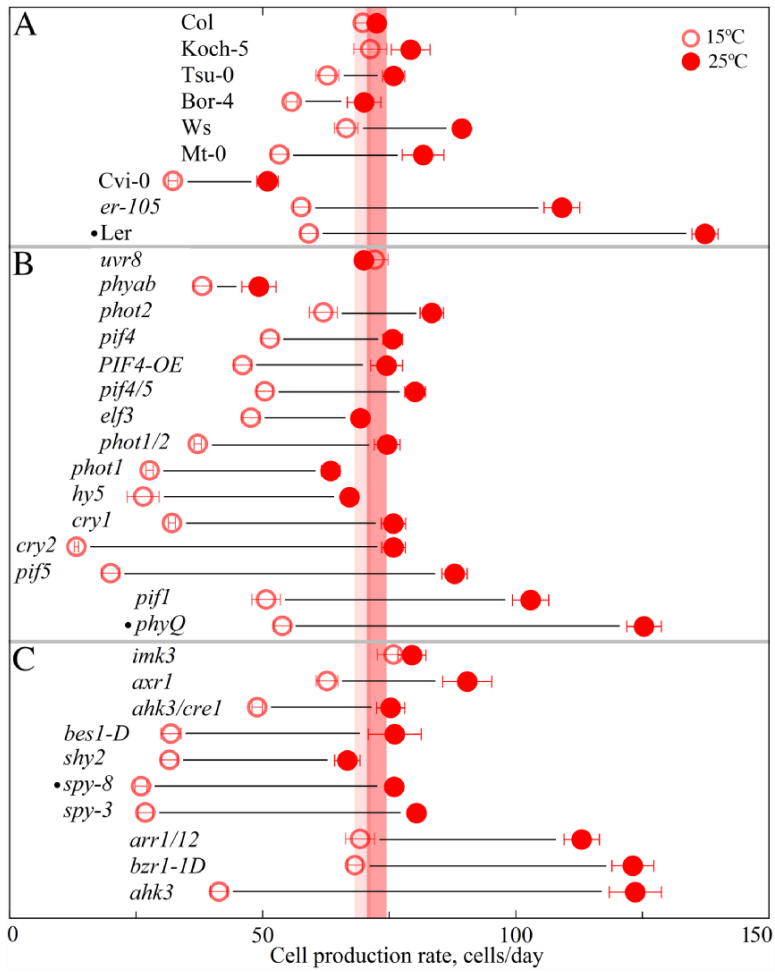

Fig. 5 Cell production rate for the indicated genotypes. (A) Accessions. (B) Photobiology related lines. (C) Developmental lines. Symbols show mean ± SD. Vertical bands are centered at the mean for Columbia and are as wide as the SD. Line names preceded by a filled circle are in the Ler background.

the variation in root growth rate was explained to a negligible extent by relative elongation rate but to an appreciable extent by growth-zone length. These results were general among the lines, but only for plants grown at 25°C; instead at 15°C, the two parameters contributed equivalently to root growth rate (**Table 1**). Thus, surprisingly, the relative contribution from relative elongation rate and growth-zone length to determining root growth rate depends on temperature.

Relationships between division and growth

Root growth rate has been considered to depend directly on the rate of cell production (Beemster and Baskin 1998). In this view, the supply of cells dictates the 'supply' of elongation because each cell is endowed with the capacity for a fixed amount of elongation. In the data obtained here, the rate of root growth was roughly correlated with the rate of cell production (**Fig. 11A**). However, the correlation was tight only for cell production rates below 30 cells/day and growth rates below 7 mm/day, the same range where a correlation was found among 18 *A. thaliana* accessions (Beemster et al. 2002). At faster rates of cell production, the correlation weakened or vanished: at 15°C, cell production rates between roughly 30 to 70 cells/day were associated with essentially the same root growth rate; at 25°C, a cloud of points clustered around 75 cells/day with considerable variation in root growth rate. What is more, there appeared to be an upper limit on root growth rate: lines with the highest rates of cell production (i.e. more than 100 cells/day) were not associated with the highest rates of root growth.

If cells flowing into the elongation zone have a cell-autonomous capacity for growth, then the rate of cell production should specify the length of the growth zone. Contradicting this prediction, growth-zone length was largely independent of cell production rate (**Fig. 12B**). These data imply that the length of the growth zone is not simply a de facto consequence of the supply of elongating cells; instead, roots are able to specify the length of the growth zone by other means.

Furthermore, cell production rate had little if any predictive value for mature cell length (**Fig. 12A**). Insofar as mature cell length depends on the length of the cell upon exiting the meristem, relative elongation rate and the length of the

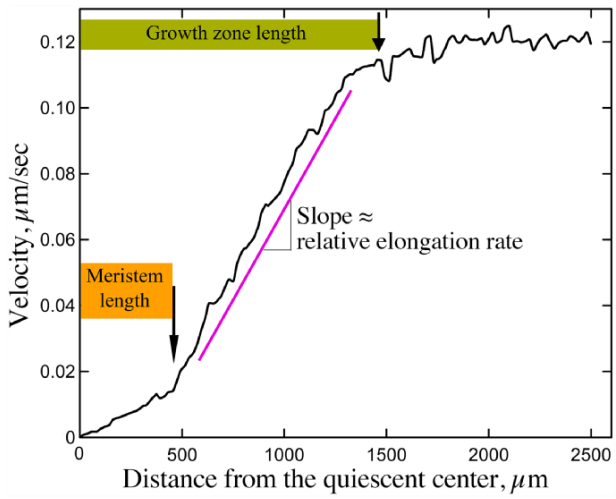

Fig. 6 Diagram illustrating parameterization of the velocity profile. The black line shows a velocity profile (Stripflow output) for an individual root. The two *x*-axis values for the two transitions (black arrows) and the relative elongation rate (solid line) were obtained by curve fitting (see Methods).

elongation zone, the lack of relationship between mature cell length and cell production rate is not surprising. For the group of lines producing more than 100 cells/day, cell length fell at the low end of the measured range: this maturation of a plentiful supply of short cells is consistent with the extent of elongation being limited by a non-cell-autonomous mechanism. The limit could reflect the mechanism that determines growth-zone length.

Also, mature cell length was not evidently correlated with root growth rate (**Fig. 12B**). Sometimes, cell length is used as a proxy to evaluate elongation rate; this practice receives no support here. Curiously, cell length ranged between 100 and 225 μm, seldom exceeding these limits. These limits are held for either temperature and are reflected in the steady-state Q_{10} for cell length never exceeding 2 (**Fig. 3**).

Finally, cell production rate was inversely correlated with meristem length (**Fig. 13**). When the data at each temperature were considered separately, there was apparently no correlation whatsoever. Although our delineation of meristem length includes a region of non-dividing cells shootward of the meristem proper (sometimes called the 'transition zone'), the length of this zone in Columbia changes in proportion to that of the actual meristem (Yang et al. 2017). Insofar as meristem length is widely assumed to reflect meristem activity, these results are surprising; however, the activity of the meristem depends on the number of dividing cells and their rate of cell division. Overall, our developmental findings are consistent with division and elongation parameters in the root being considerably independent, both in general and during thermomorphogenesis.

Discussion

Elongation and cryptochrome 2

Our results illuminate the genetic basis of thermomorphogenesis in roots. In general, we add further evidence to the idea that pathways for thermomorphogenesis differ between roots and shoots (Sanchez-Bermejo et al. 2015, Martins et al. 2017, Bellstaedt et al. 2019, Gaillochet et al. 2020, Lee et al. 2021, Borniego et al. 2022, Ai et al. 2023). In the shoot, temperature response is mediated to a considerable extent by PIF4, ELF3 and phytochrome. In root thermomorphogenesis, these genes are quiescent. Conversely, in shoots, temperature response scarcely relies on PIF5, and yet this protein appears to participate in the root, at least to some extent.

A few lines grew faster than Columbia at both temperatures and several grew slower at both temperatures, suggesting general changes to growth. Among these lines, some deviated more strongly from Columbia at one temperature than at the other. These differences might imply a specific, if subtle, connection to thermomorphogenesis; instead, they might imply an indirect consequence of the mutated pathway, a reasonable implication given that many pathways impinge on root growth (Wachsman et al. 2015, Dinneny 2019, Eljebbawi et al. 2021).

Along with phytochrome, we screened knockouts in UVR8, phototropin and cryptochrome. Further linking thermo- and photomorphogenesis, these photoreceptors too are offered as candidates for temperature sensors because their dark reversion kinetics might act similarly to those of phytochrome. In shoots, UVR8 suppresses thermomorphogenesis (Hayes et al. 2017). Phototropin mediates temperature-dependent chloroplast motility (Kodama et al. 2008, Łabuz et al. 2015, Fujii et al. 2017). Finally, cryptochrome has been connected to freezing tolerance (Imai et al. 2021, Li et al. 2021) and to temperature responses of flowering (Blázquez et al. 2003), the circadian clock (Gould et al. 2013) and shoot growth (Sanchez-Bermejo et al. 2015, Ma et al. 2016, 2021). We find that roots of all these photoreceptor mutants grew faster at 25°C than at 15°C (**Fig. 2**); evidently, for roots, these photoreceptors are neither the temperature sensor nor indispensable regulators.

Nevertheless, a cryptochrome 2 mutant was notable. At 25°C, *cry2-1* roots grew similarly to those of wild type, but at 15°C, they grew at about a fifth of the wild-type rate (**Fig. 2**). The *cry2-1* root-growth-rate phenotype was large and temperature-specific. To check whether this phenotype resulted from the loss of CRY2, we assayed another allele: a null mutant in the Ler background (*fha-1*; Koornneef et al. 1989). Compared to those of Ler, the roots of *fha-1* grew at essentially the same rate at 25°C but grew more slowly at 15°C, confirming the involvement of CRY2 in the root's response to temperature (**Supplementary Fig. S1**).

At 15°C, the *cry2* phenotype was notable in several respects. First, the line was the only one to deviate clearly from having a wild-type rate of relative elongation (**Fig. 7**). In general, the constancy of relative elongation rate among all the lines, even those where root growth rate differed substantially (e.g. *spy* and *pif5*), reveals that, in thermomorphogenesis, cell expansion is regulated robustly. Comparison with shoot growth responses to temperature is difficult because relative (i.e. cellular) expansion rate has been measured rarely.

Additionally, *cry2-1* had a short meristem at 15°C, trending even shorter than at 25°C. By contrast, the other lines resembled Columbia, having a longer meristem at 15°C than at 25°C

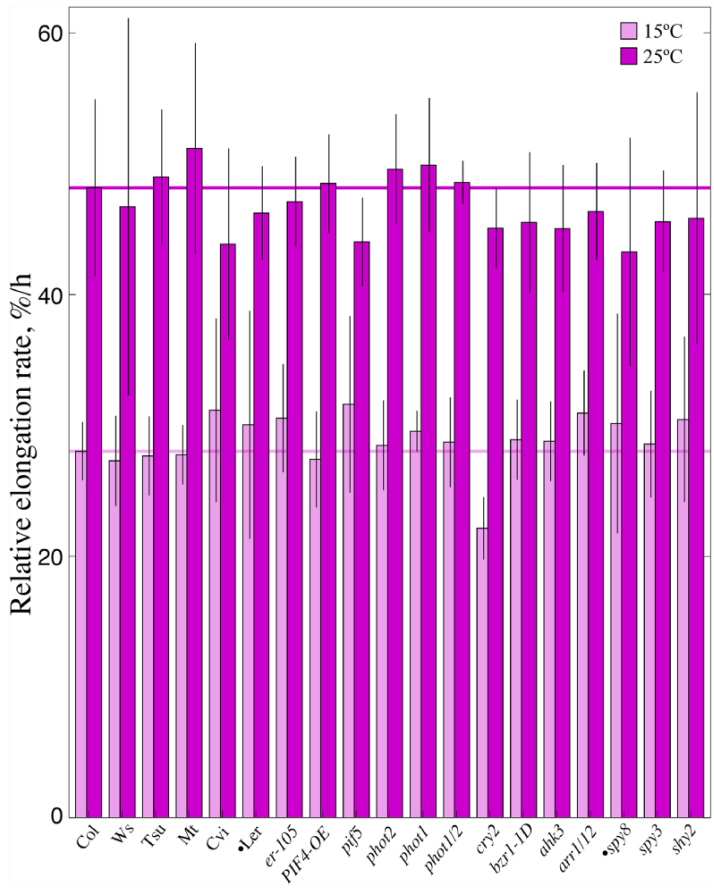

Fig. 7 Relative elongation rate at 15°C and 25°C for the indicated genotypes. Relative elongation rate is defined in **Fig. 6**. Bars show mean ± SD. Horizontal lines show the means for Columbia. All lines are in the Columbia background, except for several accessions and *spy-8* (which is in Ler; indicated by the filled circle). Sample sizes and brief descriptions are given in **Supplementary Table S1**.

(**Fig. 8**), a finding that confirms and extends previous reports (Martins et al. 2017, Yang et al. 2017, Borniego et al. 2022). These lines include mutants in genes implicated in controlling meristem length (Wachsman et al. 2015), namely, *AHK3*, *ARR1*, *ARR12* (cytokinin responses), *BZR* (brassinosteroid response) and *SHY2* (auxin). Apparently, these genes actively regulate meristem length only under certain conditions, although we cannot rule out an elaborate system that unerringly compensates the lengths of meristem proper and transition zone.

Finally, *cry2-1* had a much shorter growth zone at 15°C compared to 25°C (**Fig. 9**). This behavior stands out from all other lines, whose growth-zone lengths were more or less similar at both temperatures. Taken together, our data reveal that during thermomorphogenesis the rate at which cells elongate, the position where elongation rate speeds up and the position where it slows down are all regulated robustly. Furthermore, the specification of these attributes of elongation at 15°C depends on cryptochrome 2.

How might cryptochrome 2 be built into the machinery regulating growth rate and root zonation? Unfortunately, cryptochromes in general have been little studied in roots and work has featured cryptochrome 1 (Li and Yang 2007, Liu et al. 2011, Mishra and Khurana 2017). CRY2 is expressed in roots and the roots of *cry2* deviate from the wild type, including in growth and chlorophyll synthesis (Usami et al. 2004, Canamero et al. 2006). However, a role for the protein in root physiology has not been established. Interestingly, cryptochrome 2 sometimes acts independently of light (Yang et al. 2008, Fantini et al. 2019); furthermore, the active state of cryptochrome is longer-lived at 15°C compared to 25°C (Pooam et al. 2021). Both features are consistent with the proteins being involved in thermomorphogenesis, as are reports that cryptochromes interact with HY5 and PIFs (Ma et al. 2016, Pedmale et al. 2016, Li et al. 2021). Localizing cryptochrome 2 in roots and characterizing thermomorphogenesis in dark-grown material would be informative.

Fickle cell division

In contrast to the widespread consistency of elongation among the genotypes, cell production varied extensively (**Fig. 5**). The fine balancing act of Columbia, where cell production rate is held constant from 15°C to 25°C, was replicated in only a few of the screened lines. At 15°C, most of the genotypes produced cells more slowly than did Columbia. In some cases, this

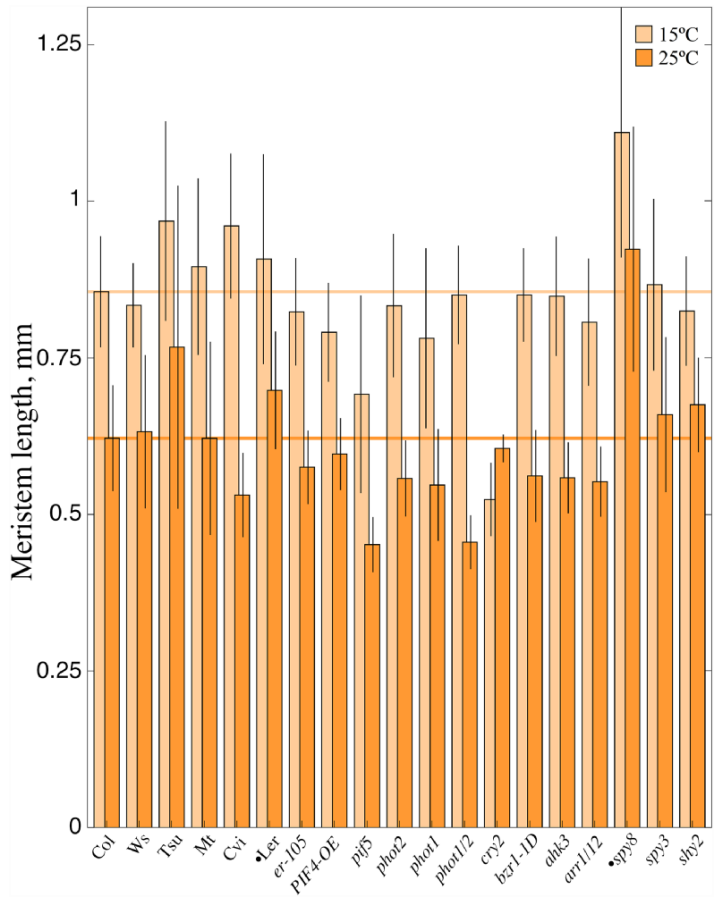

Fig. 8 Meristem length at 15°C and 25°C for the indicated genotypes. Meristem length is defined in **Fig. 6**. Bars show mean ± SD. Horizontal lines show the means for Columbia. All lines are in the Columbia background, except for several accessions and *spy-8* (which is in Ler; indicated by the filled circle). Sample sizes and brief descriptions are given in **Supplementary Table S1**.

decrease occurred with little, if any, reduced cell production at 25°C; in other cases, a decrease in cell production rate at 15°C was accompanied by an increase compared to Columbia at 25°C. Finally, a few lines produced cells notably faster at 25°C than did Columbia with little or no difference at 15°C. In root thermomorphogenesis, cell proliferation is surprisingly flexible.

One explanation for this cell division variation is that the process is regulated by pathways that are elaborate and non-redundant. Another possibility is that pathways impacting cell production are, cumulatively, metastable; if so, cell production rate would be readily disrupted in the context of even slight alterations to the metabolic status of the meristem, as conditioned by these genotypes. In this view, the altered rates of cell production reported here do not necessarily indicate specific roles in thermomorphogenesis for the wild-type gene products.

Insofar as few, if any, previous studies of thermomorphogenesis, even in shoots, quantified rates of cell production or division, we cannot readily compare our findings to others. As a proxy for cell production rate, one might consider the length of the meristem, a parameter that is widely taken to represent meristem activity. For example, in the literature on cytokinin, the longer meristems found in various mutants of genes associated with cytokinin response are interpreted as meaning that the gene products in question repress cell division (e.g. Dello Ioio et al. 2007, Argyros et al. 2008). But, as shown here, meristem length does not represent meristem activity (**Fig. 13**). As specific examples, the cell production rate of *spy-8* was remarkably low at 15°C, and yet its meristem was the longest measured; at 25°C, Landsberg had the champion cell production rate (∼130 cells/day) and a perfectly average meristem length (**Figs. 5**, **8**). Meristem length and activity should be handled as distinct, albeit connected, processes in next-generation models of root development.

Temperature invariance and root thermomorphogenesis

The rates of most developmental processes change with temperature. In fact, the rates of nearly two dozen processes ranging across spatial and temporal scales followed a similar pattern: rising with temperature to a peak and then rapidly falling (Parent and Tardieu 2012). In that context, the previous report was surprising that both cell production rate and growth-zone length were the same at 15°C and 25°C (Yang et al. 2017).

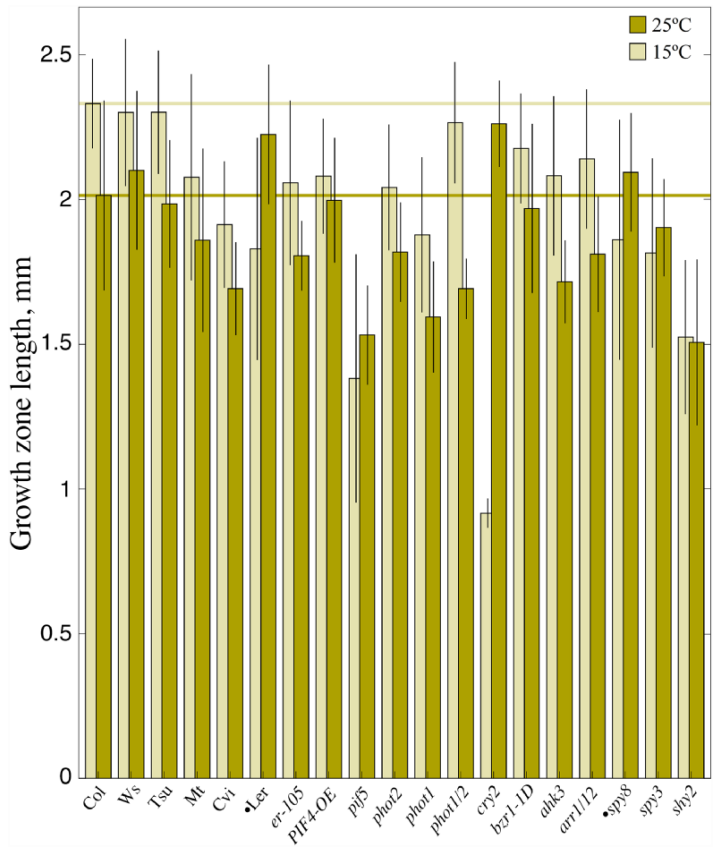

Fig. 9 Growth-zone length at 15°C and 25°C for the indicated genotypes. Growth-zone length is defined in **Fig. 6**. Bars show mean ± SD. Horizontal lines show the means for Columbia. All lines are in the Columbia background, except for several accessions and *spy-8* (which is in Ler; indicated by the filled circle). Sample sizes and brief descriptions are given in **Supplementary Table S1**.

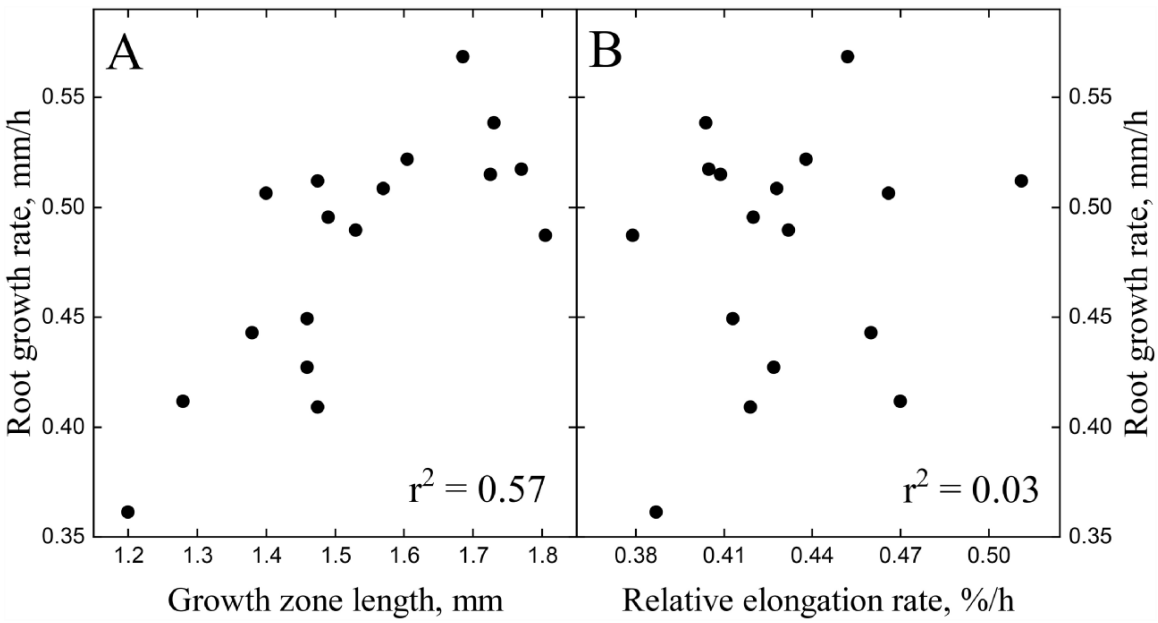

Fig. 10 Comparison of two components underlying root growth rate. Root growth rate plotted versus (A) growth-zone length and (B) relative elongation rate. Symbols are the values for each root of an example treatment (*pif5* at 25°C). Root growth rate is measured by Stripflow for a set of 80 pixels surrounding the quiescent center.

Table 1 Relationship between root growth rate, relative elongation rate and growth-zone length

Temperature (°C)	Root growth rate versus relative elongation rate r^2	Root growth rate versus growth-zone length r^2
25	0.09 ± 0.03	0.47 ± 0.06
15	0.31 ± 0.05	0.26 ± 0.06

Data are mean $\pm$ SEM, with $n = 19$ (genotypes).

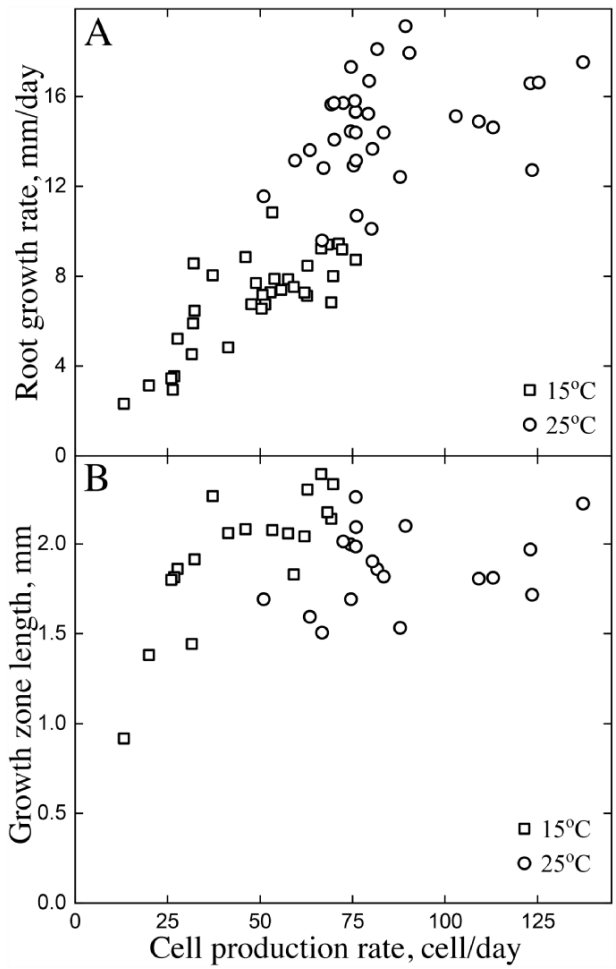

Fig. 11 Cell production rate relationships. Root growth rate (A) and growth-zone length (B) plotted versus cell production rate. Symbols represent the mean for a given treatment (i.e. genotype and temperature). Data in A are from **Figs. 2**, **5**; data in B are from **Figs. 5**, **9**.

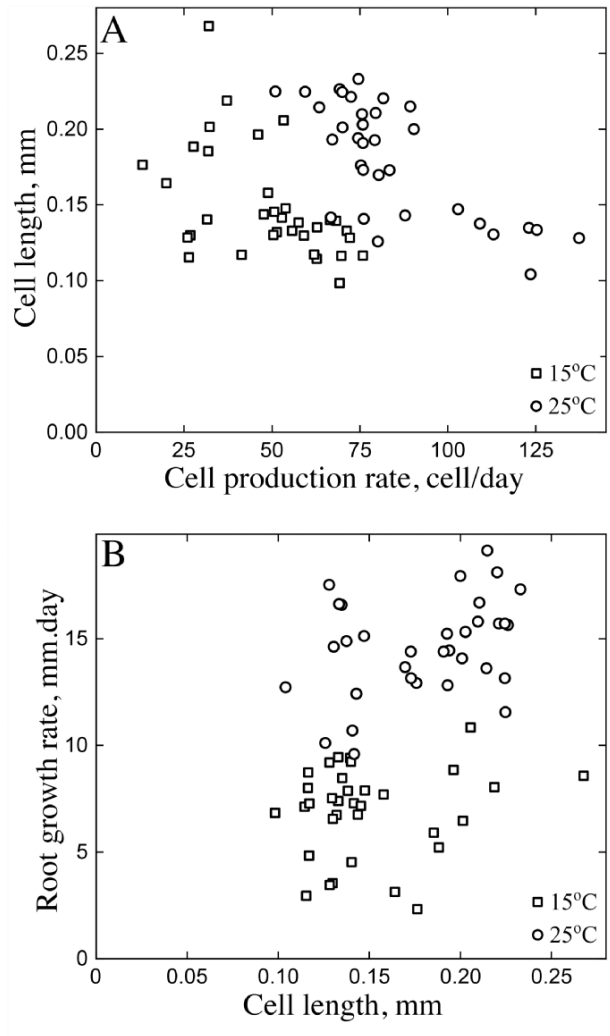

Fig. 12 Cell length relationships. Symbols represent the mean for a given treatment (i.e. genotype and temperature). Data in A are from **Figs. 4**, **5**; data in B are from **Figs. 2**, **4**.

Yang et al. (2017) hypothesized that the temperature invariance of these two processes reflected the action of a single underlying process. They argued that because the meristem supplies the elongation zone with cells, the rate of said supply determines the length of the growth zone; thus, the same rate of supply guarantees the same growth-zone length. This argument is consistent with the length of the growth zone (and hence root growth rate) increasing in lockstep with the rate of cell production during root development (Beemster and Baskin 1998) and with the correlation between rates of cell production and root growth among accessions (Beemster et al. 2002). However, the argument is inconsistent with results where stimulated cell division (by an over-expressed cyclin) fails to increase the length of the growth zone (Qi and John 2007).

Allowing the feed of cells from the meristem to determine the span of the elongation zone is an example of a cell-autonomous model, where macroscopic behavior (the shootward boundary of elongation) emerges from the independent behavior of cells (Band et al. 2012, Cole et al. 2014, Mähönen et al. 2014, Pavelescu et al. 2018). While such models are attractive in their simplicity and avoidance of spooky action-at-a-distance (as Einstein described quantum entanglement), they neglect features at the organ scale (Hervieux et al. 2016) and

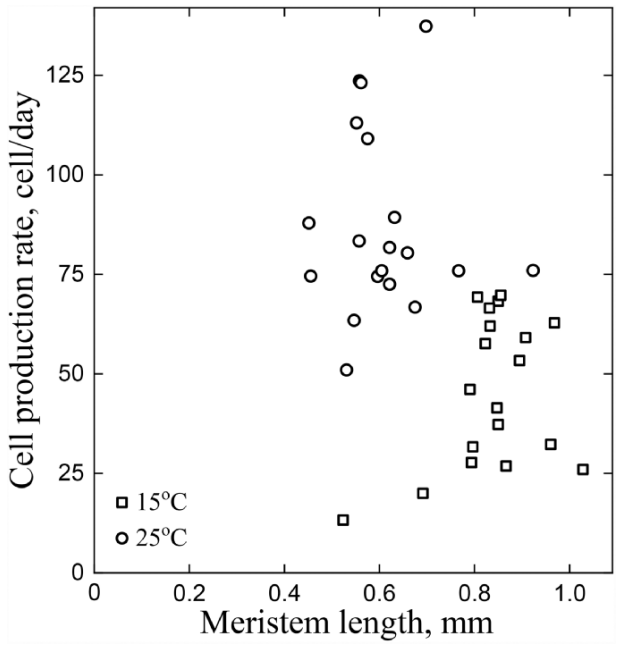

Fig. 13 Relationship between cell production rate and meristem length. Symbols represent the mean for a given treatment (i.e. genotype and temperature). Data are from **Figs. 5**, **8**.

they demand an exquisite and probably unrealistic degree of synchrony among cells (De Vos et al. 2014).

Be that as it may, Yang et al.'s hypothesis is amply refuted by the data here. Invariant growth-zone length was a feature of all but one of the lines shown, while invariant cell production rate was a feature of only a few. Our data instead support the existence of a specific mechanism to delineate the end of the elongation zone; this mechanism presumably operates even when the supply of cells and the length of the growth zone happen to both increase (as during development). The boundary at the shootward end of the elongation zone (like other boundaries within the growth zone) moves across cells as they transition from elongation to maturation; therefore, the mechanism determining its position is likely to be cell non-autonomous (Grieneisen et al. 2007). Cell-autonomous and non-autonomous programming can coexist: organ-level behavior probably reflects the integration of independent cellular behavior as modified by higher-level processes. We suggest that cryptochrome 2 will provide a route for discovering how roots build and maintain boundaries between their functional zones.

Materials and Methods

Growth conditions

Arabidopsis thaliana (L.) Heynh seeds were stored dry at 4°C or at room temperature. Seeds were surface sterilized in 15% bleach for approximately 5 min and rinsed five times with sterile water. After sterilization, seeds were sown on a modified Hoagland solution supplemented with 1% sucrose (Baskin and Wilson 1997) and solidified with 0.9% Bactoagar in 100 mm × 100 mm square Petri plates. Seeds were sewn to yield 10–13 seedlings per plate, with three plates per temperature. After sowing, seeds were stratified for 2 d at 4°C to promote germination. After stratification, plates were placed vertically in a growth chamber (Intellus LT-10, Percival, Perry, IA, USA) at either 25°C or 15°C under continuous light (80 μmol m^{-2} s^{-1}). After germination, seedlings were grown for 7 d at 25°C and 14 d at 15°C.

Accessions were obtained from the Arabidopsis Stock Center at Ohio State University. Other genotypes are in the Columbia background unless noted and were obtained as listed in the Acknowledgments. A list of all genotypes used, a brief description and an appropriate reference is given in **Supplementary Table S1**, along with sample sizes for the experiments.

Cortical cell production rate

On days 6 and 7 (25°C) or days 13 and 14 (15°C), the back of the plate was scored at the position of the root tip with a razor. After scoring the second time, the plate was scanned and the length between score marks along the root was measured (ImageJ, Schneider et al. 2012). This length divided by the time interval between the score marks gives root growth rate. After scanning, we measured the length of mature cortical cells produced by each root during the preceding 24 h. To do so, the root was cut at the first score mark and the released segment was mounted in 0.01% Triton X-100 and imaged through a compound microscope with a 20× objective lens and Nomarski optics. The length of 25–30 mature cortical cells was measured for each root. Cell production rate was calculated separately for each individual root by dividing average cell length by growth rate (Rahman et al. 2007).

Assaying elongation parameters

For characterizing elongation parameters, among the genotypes assayed for cell production rate, 18 were selected. Seedlings were grown continuously at 15°C and 25°C, as described earlier for assaying cell production rate. For imaging, a plate was transported from the growth chamber to the microscope room (~30 m distant) in an extruded polystyrene foam box containing an aluminum block, pre-equilibrated to the temperature in the growth chamber. Temperature in the microscope room was held at 25°C or 18°C, as appropriate. Although the room was not able to hold 15°C, the temperature of the agar substrate in a plate brought from the 15°C chamber to the 18°C microscope room changed by less than 1°C in 10 min. The plate was used for root imaging and returned to the growth chamber in less than10 min.

Roots were imaged through a horizontal microscope (Olympus CH2) and a 4× objective. Light from the built-in tungsten-halogen bulb passed through an IR filter and was imaged by a CCD camera (MicroEye, IDS Imaging). Image acquisition was controlled by micromanager, running a custom script to acquire four images (one every 10 s) and then a second set of four, starting 60 s after the first and also spaced every 10 s (script is available here: https://github.com/M-J-Zimmermann/Thermomorphogenesis-of-the-Arabidopsis-thaliana-root-/tree/main). In a few cases where the length of the growth zone exceeded the field of view, a second set of images was obtained after moving the stage to image the remaining part of the growth zone.

Elongation parameters were obtained from the spatial profile of velocity. Velocity profiles were obtained by using the image analysis software, Stripflow (Yang et al. 2017, Baskin and Zelinsky 2019; https://github.com/TobiasBaskin/Stripflow-release). A velocity profile was obtained from each pair of images separated by 60 s and the four profiles were averaged to represent the growth behavior of a given root. In cases where a second set of images was obtained, the average profiles were combined based on the measured overlap between image sets and the movement of tip during the time elapsed in moving the root. Elongation parameters were found by fitting the velocity profile to a modified logistic function (Peters and Baskin 2006). This function parameterizes the rate of relative elongation within the elongation zone, as well as the length of the meristem and the length of the entire growth zone.

Supplementary Data

Supplementary data are available at *PCP* online.

Data Availability

The data underlying this article are available here: https://github.com/M-J-Zimmermann/Thermomorphogenesis-of-the-Arabidopsis-thaliana-root-/tree/main.

Funding

Albert L. Delisle Scholarship (to M.J.Z.); Gilgut Fellowship (to M.J.Z.); Biology Graduate Summer Research Fellowship (to M.J.Z.); and US National Science Foundation (IOS 2035814 to T.I.B).

Acknowledgments

We thank the following former University of Massachusetts undergraduate students for invaluable technical assistance: Melissa Elmali, Jasmeen Monga, Katherine Paradis, Sofia Gaibor and Destinea Gray-Reed. We are grateful to Daniel Gibbs and Juliet Coates (both at University of Birmingham, UK) for commenting on the manuscript insightfully. We thank the following individuals for generous gift of seed: Anthony Bishopp (University of Nottingham, UK) for *cre1/ahk3*, *ahk3-3* and *arr12-1*; Peter Quail (University of California Berkeley) for *pif1-1*; Zhiyong Wang (Carnegie Institution for Plant Biology) for *bzr1-1D* and *bes1-D*; Mannie Liscum (University of Missouri Columbia) for *phot1-5/2-1*, *phot1-5* and *phot2-1*; Jia Li (University of Nanjing) for *cry1* and *cry2*; Wolfgang Busch (Salk Institute, La Jolla CA) for *PIF4-OE* and *hy5*; Phillip Wigge (Sainsbury Lab, Cambridge, UK) for *elf3-1*, *pif4-101*, *pif5* and *pif4/5*; Anderi Smertenko (Washington State University Pullman) for *imk3-1*; Hongchang Cui (University of Florida Gainsville) for *spy-3* and *spy-8*; Enamul Huq (University of Texas Austin) for *phyab*; Clark Lagarius (University of California Davis) for *phyQ* and Sourav Datta (Indian Institute of Science Education and Research, Bhopal, India) for *uvr8*.

Disclosures

The authors have no conflicts of interest to declare.

References

Ai, H., Bellstaedt, J., Bartusch, K.S., Eschen-Lippold, L., Babben, S., Balcke, G.U., et al. (2023) Auxin-dependent regulation of cell division rates governs root thermomorphogenesis. *EMBO J.* 42: e111926.

Argyros, R.D., Mathews, D.E., Chiang, Y.H., Palmer, C.M., Thibault, D.M., Etherridge, N., et al. (2008) Type B response regulators of arabidopsis play key roles in cytokinin signaling and plant development. *Plant Cell* 20: 2102–2116.

Band, L.R., Úbeda-Tomás, S., Dyson, R.J., Middleton, A.M., Hodgman, T.C., Owen, M.R., et al. (2012) Growth-induced hormone dilution can explain the dynamics of plant root cell elongation. *Proc. Natl. Acad. Sci. U. S. A.* 109: 7577–7582.

Baskin, T.I. (2013) Patterns of root growth acclimation: constant processes, changing boundaries. *WIRES Dev. Biol.* 2: 65–73.

Baskin, T.I. and Wilson, J.E. (1997) Inhibitors of protein kinases and phosphatases alter root morphology and disorganize cortical microtubules. *Plant Physiol.* 113: 493–502.

Baskin, T.I. and Zelinsky, E. (2019) Kinematic characterization of root growth by means of Stripflow. *In Plant Cell Morphogenesis: Methods and Protocols*, 2nd edn. Edited by Cvrčková, F. and Žárský, V. pp. 291–305. Springer Nature, Berlin, Germany.

Beemster, G.T.S. and Baskin, T.I. (1998) Analysis of cell division and elongation underlying the developmental acceleration of root growth in *Arabidopsis thaliana*. *Plant Physiol.* 116: 1515–1526.

Beemster, G.T.S., De Vusser, K., De Tavernier, E., De Bock, K. and Inzé, D. (2002) Variation in growth rate between Arabidopsis ecotypes is correlated with cell division and A-type cyclin-dependent kinase activity. *Plant Physiol.* 129: 854–864.

Bellstaedt, J., Trenner, J., Lippmann, R., Poeschl, Y., Zhang, X., Friml, J., et al. (2019) A mobile auxin signal connects temperature sensing in cotyledons with growth responses in hypocotyls. *Plant Physiol.* 180: 757–766.

Blázquez, M.A., Ahn, J.H. and Weigel, D. (2003) A thermosensory pathway controlling flowering time in *Arabidopsis thaliana*. *Nat. Genet.* 33: 168–171.

Borniego, M.B., Costigliolo-Rojas, C. and Casal, J.J. (2022) Shoot thermosensors do not fulfil the same function in the root. *New Phytol.* 236: 9–14.

Canamero, R.C., Bakrim, N., Bouly, J.-P., Garay, A., Dudkin, E.E., Habricot, Y., et al. (2006) Cryptochrome photoreceptors cry1 and cry2 antagonistically regulate primary root elongation in *Arabidopsis thaliana*. *Planta* 224: 995–1003.

Casal, J.J. and Balasubramanian, S. (2019) Thermomorphogenesis. *Annu. Rev. Plant Biol.* 70: 321–346.

Cole, R.A., McInally, S.A. and Fowler, J.E. (2014) Developmentally distinct activities of the exocyst enable rapid cell elongation and determine meristem size during primary root growth in Arabidopsis. *BMC Plant Biol.* 14: 386.

Dello Ioio, R., Linhares, F.S., Scacchi, E., Casamitjana-Martinez, E., Heidstra, R., Costantino, P., et al. (2007) Cytokinins determine Arabidopsis root-meristem size by controlling cell differentiation. *Curr. Biol.* 17: 678–682.

De Vos, D., Vissenberg, K., Broeckhove, J., Beemster, G.T.S. and Sun, S.X. (2014) Putting theory to the test: which regulatory mechanisms can drive realistic growth of a root. *PLoS Comput. Biol.* 10: e1003910.

Dinneny, J.R. (2019) Developmental responses to water and salinity in root systems. *Annu. Rev. Cell Dev. Biol.* 35: 239–257.

Eljebbawi, A., Guerrero, Y.C.R., Dunand, C. and Estevez, J.M. (2021) Highlighting reactive oxygen species as multitaskers in root development. *iScience* 24: 101978.

Fantini, E., Sulli, M., Zhang, L., Aprea, G., Jiménez-Gómez, J.M., Bendahmane, A., et al. (2019) Pivotal roles of cryptochromes 1a and 2 in tomato development and physiology. *Plant Physiol.* 179: 732–748.

Fujii, Y., Tanaka, H., Konno, N., Ogasawara, Y., Hamashima, N., Tamura, S., et al. (2017) Phototropin perceives temperature based on the lifetime of its photoactivated state. *Proc. Natl. Acad. Sci. U. S. A.* 114: 9206–9211.

Gaillochet, C., Burko, Y., Platre, M.P., Zhang, L., Simura, J., Willige, B.C., et al. (2020) HY5 and phytochrome activity modulate shoot-to-root coordination during thermomorphogenesis in Arabidopsis. *Development* 147: dev192625.

Gould, P.D., Ugarte, N., Domijan, M., Costa, M., Foreman, J., Macgregor, D., et al. (2013) Network balance via CRY signalling controls the

Arabidopsis circadian clock over ambient temperatures. *Mol. Syst. Biol*. 9: 650.
Gray, S.B. and Brady, S.M. (2016) Plant developmental responses to climate change. *Dev. Biol*. 419: 64–77.
Green, P.B. (1976) Growth and cell pattern formation on an axis: critique of concepts, terminology and modes of study. *Bot. Gaz*. 137: 187–202.
Grieneisen, V.A., Xu, J., Marée, A.F.M., Hogeweg, P. and Scheres, B. (2007) Auxin transport is sufficient to generate a maximum and gradient guiding root growth. *Nature* 449: 1008–1013.
Hatfield, J.L. and Prueger, J.H. (2015) Temperature extremes: effect on plant growth and development. *Weather Clim. Extrem*. 10: 4–10.
Hayes, S., Schachtschabel, J., Mishkind, M., Munnik, T. and Arisz, S.A. (2021) Hot topic: thermosensing in plants. *Plant Cell Environ*. 44: 2018–2033.
Hayes, S., Sharma, A., Fraser, D.P., Trevisan, M., Cragg-Barber, C.K., Tavridou, E., et al. (2017) UV-B perceived by the UVR8 photoreceptor inhibits plant thermomorphogenesis. *Curr. Biol*. 27: 120–127.
Hervieux, N., Dumond, M., Sapala, A., Routier-Kierzkowska, A.-L., Kierzkowski, D., Roeder, A.H.K., et al. (2016) A mechanical feedback restricts sepal growth and shape in Arabidopsis. *Curr. Biol*. 26: 1019–1028.
Ibañez, C., Poeschl, Y., Peterson, T., Bellstädt, J., Denk, K., Gogol-Döring, A., et al. (2017) Ambient temperature and genotype differentially affect developmental and phenotypic plasticity in *Arabidopsis thaliana*. *BMC Plant Biol*. 17: 114.
Imai, H., Kawamura, Y., Nagatani, A. and Uemura, M. (2021) Effects of the blue light–cryptochrome system on the early process of cold acclimation of *Arabidopsis thaliana*. *Environ. Exp. Bot*. 183: 104340.
Kodama, Y., Tsuboi, H., Kagawa, T. and Wada, M. (2008) Low temperature-induced chloroplast relocation mediated by a blue light receptor, phototropin 2, in fern gametophytes. *J. Plant Res*. 121: 441–448.
Koornneef, M., Hanhart, C.J. and van der Veen, J.H. (1989) A genetic and physiological analysis of late flowering mutants in *Arabidopsis thaliana*. *Mol. Gen. Genet*. 229: 57–66.
Larigauderie, A. and Körner, C. (1995) Acclimation of leaf dark respiration to temperature in alpine and lowland plant species. *Ann. Bot*. 76: 245–252.
Lee, S., Wang, W. and Huq, E. (2021) Spatial regulation of thermomorphogenesis by HY5 and PIF4 in *Arabidopsis*. *Nat. Commun*. 12: 3656.
Li, Q.H. and Yang, H.Q. (2007) Cryptochrome signaling in plants. *Photochem. Photobiol*. 83: 94–101.
Li, Y., Shi, Y., Li, M., Fu, D., Wu, S., Li, J., et al. (2021) The CRY2-COP1-HY5-BBX7/8 module regulates blue light-dependent cold acclimation in Arabidopsis. *Plant Cell* 33: 3555–3573.
Liu, H., Liu, B., Zhao, C., Pepper, M. and Lin, C. (2011) The action mechanisms of plant cryptochromes. *Trends Plant Sci*. 16: 684–691.
Łabuz, J., Hermanowicz, P. and Gabryś, H. (2015) The impact of temperature on blue light induced chloroplast movements in *Arabidopsis thaliana*. *Plant Sci*. 239: 238–249.
Ma, D., Li, X., Guo, Y., Chu, J., Fang, S., Yan, C., et al. (2016) Cryptochrome 1 interacts with PIF4 to regulate high temperature-mediated hypocotyl elongation in response to blue light. *Proc. Natl. Acad. Sci. U. S. A*. 113: 224–229.
Ma, L., Li, X., Zhao, Z., Hao, Y., Shang, R., Zeng, D., et al. (2021) Light-Response Bric-A-Brack/Tramtrack/Broad proteins mediate cryptochrome 2 degradation in response to low ambient temperature. *Plant Cell* 33: 3610–3620.
Mähönen, A.P., ten Tusscher, K., Siligato, R., Smetana, O., Díaz-Triviño, S., Salojärvi, J., et al. (2014) PLETHORA gradient formation mechanism separates auxin responses. *Nature* 515: 125–129.
Martins, S., Montiel-Jorda, A., Cayrel, A., Huguet, S., Paysant-Le Roux, C., Ljung, K., et al. (2017) Brassinosteroid signaling-dependent root responses to prolonged elevated ambient temperature. *Nat. Commun*. 8: 309.
Mishra, S. and Khurana, J.P. (2017) Emerging roles and new paradigms in signaling mechanisms of plant cryptochromes. *Crit. Rev. Plant Sci*. 36: 89–115.
Noguchi, M. and Kodama, Y. (2022) Temperature sensing in plants: on the dawn of molecular thermosensor research. *Plant Cell Physiol*. 63: 737–743.
Parent, B. and Tardieu, F. (2012) Temperature response of developmental processes have not been affected by breeding in different ecological areas for 17 crop species. *New Phytol*. 194: 760–774.
Pavelescu, I., Vilarrasa-Blasi, J., Planas-Riverola, A., González-García, M.P., Caño-Delgado, A.I. and Ibañes, M. (2018) A sizer model for cell differentiation in *Arabidopsis thaliana* root growth. *Mol. Syst. Biol*. 14: e7687.
Pedmale, U.V., Huang, S.C., Zander, M., Cole, B.J., Hetzel, J., Ljung, K., et al. (2016) Cryptochromes interact directly with PIFs to control plant growth in limiting blue light. *Cell* 164: 233–245.
Peters, W.S. and Baskin, T.I. (2006) Tailor-made composite functions as tools in model choice: the case of sigmoidal vs bi-linear growth profiles. *Plant Methods* 2: 12.
Pooam, M., Dixon, N., Hilvert, M., Misko, P., Waters, K., Jourdan, N., et al. (2021) Effect of temperature on the Arabidopsis cryptochrome photocycle. *Physiol. Plant*. 172: 1653–1661.
Qi, R. and John, P.C.L. (2007) Expression of genomic *AtCYCD2;1* in *Arabidopsis* induces cell division at smaller cell sizes: implications for the control of plant growth. *Plant Physiol*. 144: 1587–1597.
Rahman, A., Bannigan, A., Sulaman, W., Pechter, P., Blancaflor, E.B. and Baskin, T.I. (2007) Auxin, actin, and growth of the *Arabidopsis thaliana* primary root. *Plant J*. 50: 514–528.
Samtani, H., Sharma, A., Khurana, J. and Khurana, P. (2022) Thermosensing in plants: deciphering the mechanisms involved in heat sensing and their role in thermoresponse and thermotolerance. *Environ. Exp. Bot*. 203: 105041.
Sanchez-Bermejo, E., Zhu, W., Tasset, C., Eimer, H., Sureshkumar, S., Singh, R., et al. (2015) Genetic architecture of natural variation in thermal responses of Arabidopsis. *Plant Physiol*. 169: 647–659.
Schneider, C.A., Rasband, W.S. and Eliceiri, K.W. (2012) NIH image to ImageJ: 25 years of image analysis. *Nat. Methods* 9: 671–675.
Silk, W.K. (1984) Quantitative descriptions of development. *Annu. Rev. Plant Physiol*. 35: 479–518.
Silk, W.K., Lord, E.M. and Eckard, K.J. (1989) Growth patterns inferred from anatomical records. Empirical tests using longisections of roots of *Zea mays* L. *Plant Physiol*. 90: 708–713.
Stoller, E.W. and Woolley, J.T. (1983) The effects of light and temperature on yellow nutsedge (*Cyperus esculentus*) basal-bulb formation. *Weed Sci*. 31: 148–152.
Thines, B., Harmon, F.G. and Kay, S.A. (2010) Ambient temperature response establishes ELF3 as a required component of the core *Arabidopsis* circadian clock. *Proc. Natl. Acad. Sci. U. S. A*. 107: 3257–3262.
Torii, K.U., Mitsukawa, N., Oosumi, T., Matsuura, Y., Yokoyama, R., Whittier, R.F., et al. (1996) The *Arabidopsis ERECTA* gene encodes a putative receptor protein kinase with extracellular leucine-rich repeats. *Plant Cell* 8: 735–746.
Usami, T., Mochizuki, N., Kondo, M., Nishimura, M. and Nagatani, A. (2004) Cryptochromes and phytochromes synergistically regulate Arabidopsis root greening under blue light. *Plant Cell Physiol*. 45: 1798–1808.

Wachsman, G., Sparks, E.E. and Benfey, P.N. (2015) Genes and networks regulating root anatomy and architecture. *New Phytol*. 208: 26–38.

Yang, X., Dong, G., Palaniappan, K., Mi, G.H. and Baskin, T.I. (2017) Temperature-compensated cell production rate and elongation zone length in the roots of *Arabidopsis thaliana*. *Plant Cell Environ*. 40: 264–276.

Yang, Y.J., Zuo, Z.C., Zhao, X.Y., Li, X., Klejnot, J., Li, Y., et al. (2008) Blue-light-independent activity of *Arabidopsis* cryptochromes in the regulation of steady-state levels of protein and mRNA expression. *Mol. Plant* 1: 167–177.

Zhang, H., Zhu, J., Gong, Z. and Zhu, J. (2021) Abiotic stress responses in plants. *Nat. Rev. Genet*. 23: 104–119.

Zimmermann, M.J., Bose, J., Kramer, E.M., Atkin, O.K., Tyerman, S.D. and Baskin, T.I. (2022) Oxygen uptake rates have contrasting responses to temperature in the root meristem and elongation zone. *Physiol. Plant*. 174: e13682.